Conserved function of the lysine-based KXD/E motif in Golgi retention for endomembrane proteins among different organisms

Cheuk Hang Woo[a],*, Caiji Gao[a],*, Ping Yu[b], Linna Tu[b], Zhaoyue Meng[c], David K. Banfield[b], Xiaoqiang Yao[c,d], and Liwen Jiang[a,d]
[a]Centre for Cell and Developmental Biology and State Key Laboratory of Agrobiotechnology, School of Life Sciences, and [c]School of Biomedical Sciences, Chinese University of Hong Kong, Shatin, New Territories, Hong Kong, China; [b]Division of Life Science, Hong Kong University of Science and Technology, Clear Water Bay, Kowloon, Hong Kong, China; [d]CUHK Shenzhen Research Institute, Chinese University of Hong Kong, Shenzhen 518057, China

ABSTRACT We recently identified a new COPI-interacting KXD/E motif in the C-terminal cytosolic tail (CT) of *Arabidopsis* endomembrane protein 12 (AtEMP12) as being a crucial Golgi retention mechanism for AtEMP12. This KXD/E motif is conserved in CTs of all EMPs found in plants, yeast, and humans and is also present in hundreds of other membrane proteins. Here, by cloning selective EMP isoforms from plants, yeast, and mammals, we study the localizations of EMPs in different expression systems, since there are contradictory reports on the localizations of EMPs. We show that the N-terminal and C-terminal GFP-tagged EMP fusions are localized to Golgi and post-Golgi compartments, respectively, in plant, yeast, and mammalian cells. In vitro pull-down assay further proves the interaction of the KXD/E motif with COPI coatomer in yeast. COPI loss of function in yeast and plants causes mislocalization of EMPs or KXD/E motif–containing proteins to vacuole. Ultrastructural studies further show that RNA interference (RNAi) knockdown of coatomer expression in transgenic *Arabidopsis* plants causes severe morphological changes in the Golgi. Taken together, our results demonstrate that N-terminal GFP fusions reflect the real localization of EMPs, and KXD/E is a conserved motif in COPI interaction and Golgi retention in eukaryotes.

INTRODUCTION

In eukaryotic cells, secretory proteins are synthesized in the rough endoplasmic reticulum (ER) and then transported to the Golgi apparatus mediated by the coat protein complex II (COPII) for further modification and sorting to post-Golgi compartments, including the *trans*-Golgi network (TGN) and multivesicular bodies (MVBs),

identified as prevacuolar compartments (PVCs) in plant cells (Barlowe *et al.*, 1994; Tse *et al.*, 2004). Resident proteins in the early secretory pathway can be retrieved back to the ER or be retained in the Golgi to ensure the structural integrity and normal function of these organelles. Specific sorting signals and transport machineries are responsible for the retrieval or retention of these resident proteins. For instance, the C-terminal KKXX motif, which has been identified in many ER-localized type I membrane proteins, can function as an ER retention signal to retrieve ER-resident membrane proteins from the Golgi via a direct interaction with coat protein complex I (COPI) coatomers (Cosson and Letourneur, 1994; Letourneur *et al.*, 1994; Contreras *et al.*, 2004). Another example is the semiconserved (F/L)-(L/V)-(S/T) motif, which has been shown to function as Golgi retention signal by interacting with COPI vesicles via Vps74p, thereby maintaining the steady Golgi localization of glycosyltransferases in yeast (Tu *et al.*, 2008).

Endomembrane proteins (EMPs) are a family of integral proteins with a large lumenal N-terminus, nine transmembrane domains,

A Protein   Localization

Protein	Localization
AtEMP12	Golgi
GFP-AtEMP12	Golgi
AtEMP12-GFP	Post-Golgi (TGN, PVC, vacuole)

COPII interaction   COPI interaction

S N L F V R R I Y R N I K C D

B AtEMP12

COOH
Cytosol
Membrane
Lumen
NH2 SP
TMD TMD TMD TMD TMD

GFP-AtEMP12

COOH
Cytosol
Membrane
Lumen
NH2 SP GFP
TMD TMD TMD TMD TMD

AtEMP12-GFP

GFP COOH
Cytosol
Membrane
Lumen
NH2 SP
TMD TMD TMD TMD TMD

COPII interaction   COPI interaction

C

AtEMP1	633	A	C	L	W	F	T	R	L	I	Y	S	S	V	K	I	D	648	
AtEMP2	629	A	C	L	W	F	T	R	L	I	Y	S	S	V	K	I	D	644	
AtEMP3	622	A	C	F	W	F	T	R	L	I	Y	S	S	V	K	I	D	637	
AtEMP4	622	A	C	L	W	F	V	R	K	I	Y	S	S	V	K	I	D	637	
AtEMP5	627		C	F	W	F	V	R	K	I	Y	S	S	V	K	I	D	641	
AtEMP6	615	S	S	F	W	F	V	H	Y	L	F	S	S	V	K	L	D	630	
AtEMP7	640				Y	F	V	H	Y	L	F	S	S	V	K	I	D	652	
AtEMP8	579			L	L	F	V	R	H	I	Y	R	S	I	K	C	E	592	
AtEMP9	579			L	L	F	V	R	H	I	Y	R	S	I	K	C	E	592	*
AtEMP10	580			L	L	F	V	R	H	I	Y	R	S	I	K	C	E	593	*
AtEMP11	496				M	F	I	R	H	I	Y	R	S	V	K	L	E	508	
AtEMP12	575			S	N	L	F	V	R	R	I	Y	R	N	I	K	C	D	589
HsTM9SF1	593				L	K	F	I	R	Y	I	Y	V	N	L	K	M	D	606	*
HsTM9SF2	651				W	F	V	T	K	I	Y	S	V	V	K	V	D	663	
HsTM9SF3	576			S	A	F	V	R	K	I	Y	T	N	V	K	I	D	589	
HsTM9SF4	630				M	F	V	R	K	I	Y	A	A	V	K	I	D	642	*
ScTMN1	652	S	S	M	L	F	V	R	K	I	Y	S	S	I	K	V	D	667	*
ScTMN2	656	F	S	S	M	F	F	I	R	K	I	Y	S	A	I	K	V	E	672	*
ScTMN3	690	L	T	A	S	W	F	I	N	K	I	Y	H	Q	K	V	N	L	706

FIGURE 1: Topology and sequence analysis of EMP family proteins. (A) Localization summary of AtEMP12 and its fusions in a plant expression system. (B) Schematic topology of AtEMP12 predicted by TMHMM 2.0 and construction of GFP-AtEMP12 and AtEMP12-GFP fusions. (C) Alignment of C-terminal sequences of EMP family from *A. thaliana* (At), *S. cerevisiae* (Sc), and *Homo sapiens* (Hs).

2010). Nevertheless, the C-terminal myc-tagged EMPs and the endogenous EMPs recognized by anti-HsTM9SF4 antibody in mammalian cells were found to be localized to endosomes (Schimmöller *et al.*, 1998; Lozupone *et al.*, 2009), whereas the C-terminal GFP-tagged HsTM9SF1-GFP localized to autophagosomes and lysosomes (He *et al.*, 2009). In a more recent study on plants, AtEMP12-specific antibodies, as well as stably or transiently expressed fluorescently tagged fusions, were used (Gao *et al.*, 2012). As a result, both endogenous AtEMP12 and an N-terminal tagged GFP-AtEMP12 fusion were found to localize exclusively to the Golgi apparatus (Gao *et al.*, 2012). By contrast, the C terminal–fused GFP tag caused mislocalization of the AtEMP12-GFP fusion to post-Golgi compartments and vacuoles for degradation (Gao *et al.*, 2012). By mutagenesis analysis, a new lysine-based KXD/E motif in the C-terminal CT of AtEMP12 was shown to be crucial for COPI binding and Golgi retention of AtEMP12 (Gao *et al.*, 2012).

Of interest, this KXD/E motif seems to be highly conserved in the CT of numerous EMP isoforms, including the 12 members (AtEMP1 to AtEMP12) of *Arabidopsis*, the four members (HsTM9SF1 to HsTM9SF4) in humans, and the two members (ScTMN1 and ScTMN2) in yeast (Gao *et al.*, 2012, 2014a). In addition, the KXD/E motif can also be found in many membrane proteins of unknown localization information among different organisms (Gao *et al.*, 2014a). Here we characterize the subcellular localizations of selective EMPs among different organisms and examine the conserved function of the KXD/E motif. We demonstrate that the selective EMPs from plants, yeasts, and animals all localized to the Golgi when the XFP tag was fused to the N-terminus, whereas C-terminal XFP-tagged EMP fusions mislocalized to post-Golgi compartments and the vacuole. We further show that the KXD/E motif could also bind to coatomer in yeast, indicating that N-terminal GFP-tagged EMPs can reflect the real localization of EMPs. In addition, dysfunction of COPI function via temperature-sensitive mutation of coatomer in yeast or inducible RNA interference (RNAi) knockdown of coatomer in plants results in a mislocalization EMPs to the vacuole, suggesting a conserved retention function and COPI-binding ability of KXD/E motif in the Golgi apparatus of different eukaryotes.

RESULTS

KXD/E motif confers Golgi localization of EMP homologues in plants, mammals, and yeast

We recently identified dual sorting signals including the COPII interaction motif, FV/Y, and the COPI interaction motif, KXD/E, in the C-terminal cytosolic tail of AtEMP12 as being essential for maintaining Golgi localization of *Arabidopsis* EMPs (Figure 1; Gao *et al.*, 2012). EMP isoforms can also be found in yeast (*S. cerevisiae*) and humans (*H. sapiens*), and the lysine-based KXD/E motif seems to be

and a short cytoplasmic tail (CT). Originally identified in humans (*Homo sapiens*; HsTM9SF1 to HsTM9SF4; Chluba-de Tapia *et al.*, 1997; Schimmöller *et al.*, 1998; Lozupone *et al.*, 2009), the EMP family has also been found in various organisms, including the 12 members in *Arabidopsis* (AtEMP1 to AtEMP12; Gao *et al.*, 2012), three members in yeast (*Saccharomyces cerevisiae*; ScTMN1 to ScTMN3; Froquet *et al.*, 2008), and three members in *Dictyostelium discoideum* (Phg1A to Phg1C; Cornillon *et al.*, 2000). Phg1A and Phg1B in *D. discoideum* were discovered to contribute to cellular adhesion and phagocytosis (Benghezal *et al.*, 2003). Phg1A and Phg1B were later revealed to be involved in efficient intracellular killing of bacteria (Le Coadic *et al.*, 2013). ScTMN was reported to contribute to cell adhesion and filamentous growth of nitrogen-starved yeast (Froquet *et al.*, 2008). Moreover, high expression levels of the EMP HsTM9SF4 in human malignant metastatic melanoma cells suggested that HsTM9SF4 could act as a malignancy marker (Lozupone *et al.*, 2009).

Controversy surrounds the subcellular localizations of EMPs. For example, yeast EMP ScTMN3 was found in Golgi, whereas C-terminal green fluorescent protein (GFP)–tagged ScTMN2 was localized to endosomes and the vacuole (Huh *et al.*, 2003; Aguilar *et al.*,

Gene	Fusion Protein		Expression System
	Protein Name	Construct	
Plant			
AtEMP9	GFP-AtEMP9	sp-GFP / AtEMP9	P
	AtEMP9-GFP	AtEMP9 / GFP	P
AtEMP10	GFP-AtEMP10	sp-GFP / AtEMP10	P
	AtEMP10-GFP	AtEMP10 / GFP	P
AtEMP12	GFP-AtEMP12	sp-GFP / AtEMP12	M
	AtEMP12-GFP	AtEMP12 / GFP	M
Mammal			
HsTM9SF1	GFP-HsTM9SF1	sp-GFP / HsTM9SF1	M, P
	HsTM9SF1-GFP	HsTM9SF1 / GFP	M, P
HsTM9SF4	GFP-HsTM9SF4	sp-GFP / HsTM9SF4	M, P
	HsTM9SF4-GFP	HsTM9SF4 / GFP	M, P
Yeast			
ScTMN1	XFP-ScTMN1	sp-XFP / ScTMN1	Y, M, P
	ScTMN1-XFP	ScTMN1 / XFP	Y, M, P
ScTMN2	GFP-ScTMN2	sp-XFP / ScTMN2	M, P
	ScTMN2-GFP	ScTMN2 / GFP	M, P

FIGURE 2: Summary of the constructs and expression systems used in this study. The cloned EMPs and their XFP fusions used in this study. These various XFP fused EMPs are expressed in either their original or the heteroexpression system. M, mammal; P, plant; Y, yeast.

conserved in all of these isoforms, with the exception of the yeast ScTMN3 (Figure 1). To test the possible conserved function of this lysine-based KXD/E sorting signal, we cloned selective EMPs from various model organisms and made GFP fusions at the N- or the C-terminus to study their subcellular localization (Figure 2 and Supplemental Figure S1).

We first tested the localizations of various GFP fusions of EMP homologues in their original expression system. As shown in Figure 3A and Supplemental Figure S2A, N-terminal GFP fusions of At-EMP9 and AtEMP10 showed correct Golgi localizations for plant EMPs expressed in plant cells. However, localizations of the C-terminal GFP fusion proteins were shifted, as AtEMP9-GFP and AtEMP10-GFP signals localized to vacuole and punctate structures distinct from the Golgi marker ManI-mRFP (Figure 3A and Supplemental Figure S2A). The correct expressions and integrity of GFP fusions of AtEMP9 and AtEMP10 were further confirmed by Western blot analysis with GFP antibodies (Supplemental Figure S3). These results demonstrate that AtEMP9 and AtEMP10 share similar localization patterns upon GFP fusions at N- or C-terminus to the corresponding GFP fusions of AtEMP12 reported previously (Gao et al., 2012), indicating a general targeting mechanism for the EMPs in *Arabidopsis* plants.

To study the subcellular localizations of *H. sapiens* EMP homologues in mammalian cells, we first used HsTM9SF4 antibody to detect the localization of endogenous HsTM9SF4 in HEK293a cells by performing confocal immunofluorescence labeling. As shown in Figure 3B, anti-HsTM9SF4 antibody recognized and colocalizes with GFP-HsTM9SF4 (Figure 3B). In addition, a large portion of the en-

dogenous HsTM9SF4 in HEK293a cells showed perinuclear aggregations that were largely colocalized with the Golgi marker anti-GM130 (Figure 3B). At a first glance, this result seems to be contradicted by a previous report, which demonstrated endosomal localization of endogenous HsTM9SF4 in metastatic melanoma cells (Lozupone et al., 2009). However, we noticed that the HEK293a cells used in our experiments are derived from human embryonic kidney, whereas the metastatic melanoma cells used in the previous study were cancer cells (Lozupone et al., 2009). We suspect that such different localizations of HsTM9SF4 observed in this study and the previous report could be due to different types of cell lines used. Indeed, we observed different staining patterns with anti-HsTM9SF4 antibody in normal cells (HEK293a) versus in cancer cells (MCF-7), as shown in Supplemental Figure S4.

We next cloned the *H. sapiens* EMP homologues and made various GFP fusions for the localization study in mammalian cells. The N-terminal GFP-fused GFP-HsTM9SF4 and GFP-HsTM9SF1 mostly localized to the Golgi apparatus, as it showed perinuclear aggregations that were typical for the Golgi marker anti-GM130 (Figure 3B and Supplemental Figure S2, B and C). Nevertheless, localization of the C-terminal GFP-fused HsTM9SF4-GFP and HsTM9SF1-GFP was shifted from the Golgi to post-Golgi endo-

somal compartments (Figure 3B and Supplemental Figure S2, B and C). The correct expression and integrity of N- and C-terminal GFP-tagged HsTM9SF4 in mammalian cells were further confirmed by Western blot analysis with GFP antibody (Supplemental Figure S3). If we compare the expression of N- or C-terminal GFP fusions of HsTM9SF4 in mammalian cells with the corresponding GFP fusions of AtEMPs in plants, we find similar expression patterns, as the N-terminal GFP fusions always localized to the Golgi, whereas the C-terminal GFP fusions shifted localization to the post-Golgi compartments.

A subcellular localization study of the *S. cerevisiae* EMP homologue was also conducted in yeast. The N terminal–tagged EmCit-ScTMN1 showed a typical punctate Golgi pattern and was largely colocalized with the Golgi marker Bet1p-mRFP in yeast cells, but the localization signal was obviously shifted to vacuole when the fluorescent tag was fused to the C-terminus of TMN1 (Figure 3C).

To prove further the essential function of the KXD/E motif in mediating Golgi retention of EMPs, we next made point mutations of the KXD/E motif in selected EMPs from plants, yeast, and mammals and generated the N-terminal GFP fusions of these mutated EMPs for localization study. The results demonstrated that mutation of the KXD/E motif caused the localization shift of the N terminal–tagged GFP-EMP fusions from the Golgi apparatus to other compartments in plant, mammalian, and yeast cells (Supplemental Figure S4). Taken together, these results demonstrate similar localization patterns of different EMP homologues from different organisms and thus suggest a conserved function of the KXD/E motif in maintaining Golgi localization of EMPs in eukaryotes.
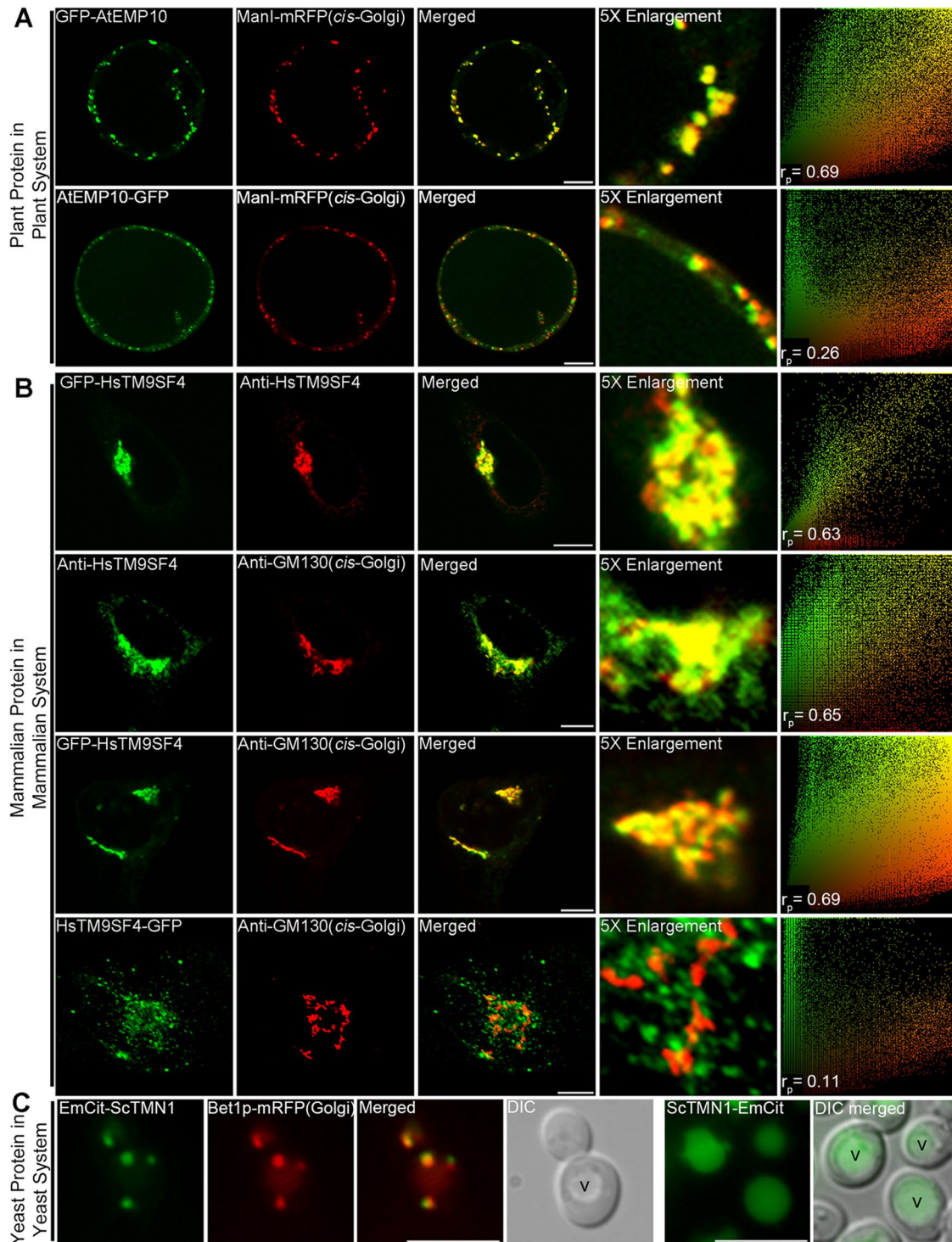
FIGURE 3: Localizations of EMP family proteins in their native expression systems. (A) GFP-AtEMP10 and AtEMP10-GFP were coexpressed with the *cis*-Golgi marker ManI-mRFP in *Arabidopsis* protoplasts, followed by confocal imaging at 12–14 h after transfection. Far right, colocalization relationship shown with Pearson–Spearman correlation. Bars, 10 μm. (B) Typical subcellular localization patterns of endogenous HsTM9SF4, GFP-HsTM9SF4, and HsTM9SF4-GFP in HEK293a cells. The indicated cells with or without transfection were immunolabeled with antibodies of *cis*-Golgi protein GM130 or HsTM9SF4, followed by confocal imaging. Colocalization relationship was calculated by Pearson–Spearman correlation. Bars, 10 μm. (C) Typical subcellular localization patterns of EmCit-ScTMN1 and ScTMN1-EmCit after transformation and selection, followed by imaging under a fluorescence microscope after incubation in YEPD for 3–5 h. V, vacuoles in yeast. Bars, 10 μm.
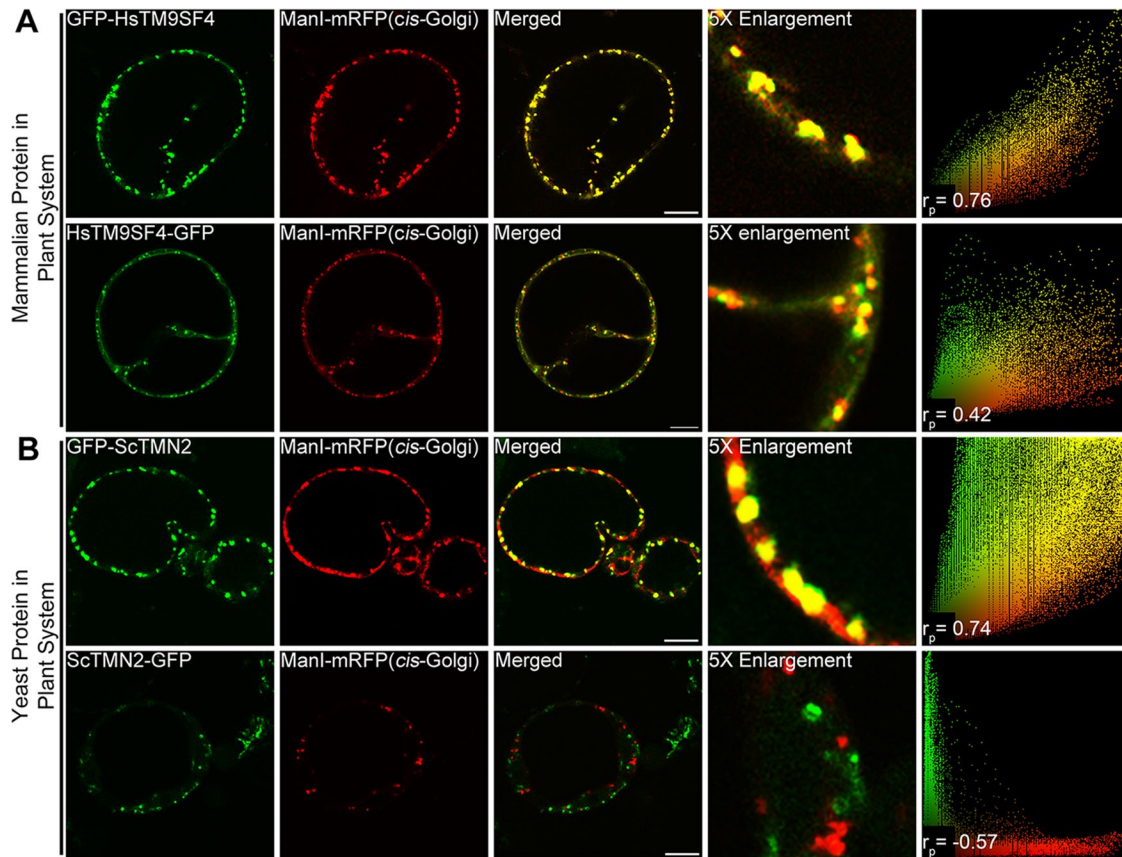
FIGURE 4: Localizations of foreign EMP family proteins in plant expression system. (A) Typical subcellular localization patterns of GFP-HsTM9SF4 and HsTM9SF4-GFP coexpressing with *cis*-Golgi marker ManI-mRFP in *Arabidopsis* protoplasts, followed by confocal imaging 12–14 h after transfection. Analysis of colocalization relationship using Pearson–Spearman correlation. Bars, 10 μm. (B) Coexpressions of GFP-ScTMN2 and ScTMN2-GFP with *cis*-Golgi marker ManI-mRFP performed in *Arabidopsis* protoplasts. Confocal images of transfected cells were collected after 12–14 h of transfection. Colocalization relationship was measured using Pearson–Spearman correlation. Bars, 10 μm.

Localization patterns of EMP homologues in a heteroexpression system are similar to their localization in a native expression system

In addition to expressing EMP homologues among different organisms expressed in their native expression systems, the heteroexpression of foreign EMP homologues was also carried out to investigate further the conserved functions of the KXD/E motif. We first investigated the localizations of EMP homologues from mammals and yeast after expression in plant cells. As shown in Figure 4, the N-terminal GFP fusions of mammalian and yeast EMP homologues (HsTM9SF4 and ScTMN2, respectively) showed Golgi localization in the plant cell, whereas those homologues with GFP fused to the C-terminus resulted in a localization shift from the Golgi. Similar localization patterns were detected with HsTM9SF1 and ScTMN1 when expressed in plant cells (Supplemental Figure S5, A and B). In addition to the expression of mammalian and yeast EMP homologues in the plant cell, we also explored the localizations of plant and yeast EMP homologues after expression in a mammalian cell. Once again, the N-terminal GFP fusions of AtEMP12 and ScTMN1 showed *cis*-Golgi localization in the mammalian system (Figure 5, A and B). As before, when the GFP was fused at the C-terminus of AtEMP12 and ScTMN1, their localizations were shifted from *cis*-Golgi to post-Golgi compartments such as early endosomes (Figure 5, A and B). Similar localization patterns were also observed with ScTMN2 when expressed in mammalian cells (Supplemental Figure S5C). The

foregoing experiments demonstrate the Golgi localizations of N-terminal XFP-fused EMP isoforms when expressed in heteroexpression systems, further proving the conserved role of the KXD/E motif in conferring Golgi retention of EMPs among different organisms.

Conserved COPI binding and Golgi retention properties of KXD/E motif in yeast

We previously showed that the KXD/E motif binds COPI coatomers to retain AtEMP12 in the Golgi of *Arabidopsis* (Gao *et al.*, 2012). To examine whether the KXD/E motif has similar COPI-binding ability in other organisms, we used synthetic peptides corresponding to the AtEMP12 CT as bait to perform pull-down assays using proteins from yeast cell extracts followed by SDS–PAGE separation and tandem mass spectrometry (MS/MS) analysis for protein identification (Figure 6A). As shown in Figure 6, B and C, the wild-type AtEMP12 CT peptide but not the mutated one pulled out the COPI coat subunits β-COP and ε-COP. This result is consistent with our previous pull-down study using *Arabidopsis* proteins (Gao *et al.*, 2012), indicating a conserved interaction ability of the KXD/E motif and COPI coatomer from different organisms.

The COPI-binding ability of the KXD/E motif in yeast prompted us to examine further whether this COPI-interacting motif has a similar Golgi retention effect in other yeast membrane proteins. We next used a gain-of-function approach by adding the KXD/E motif to the C-terminus of vacuole-targeted GFP-Rer1p-Δ10. Rer1p is a
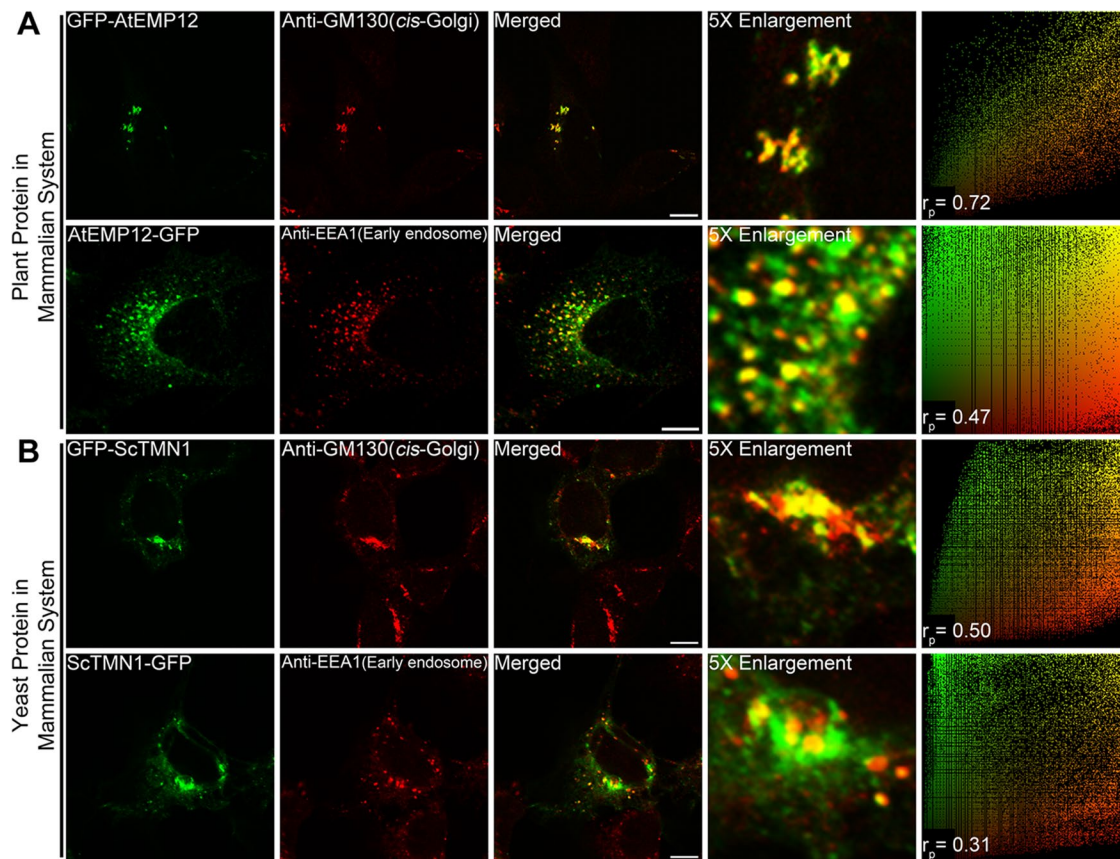
FIGURE 5: Localizations of foreign EMP family proteins in mammalian expression system. (A) Typical subcellular localization patterns of GFP-AtAtEMP12 and AtAtEMP12-GFP after 12-14h of transfection in HEK293a cells. Transfected cells were immunolabeled with antibody of *cis*-Golgi protein GM130 or early endosome protein EEA1 before confocal imaging. Colocalization relationship was depicted by Pearson–Spearman correlation. Bars, 10 μm. (B) Representative subcellular localization of GFP-ScTMN1 and ScTMN1-GFP in HEK293a cells. Cells transfected for 12–14 h were then immunolabeled with antibody of *cis*-Golgi protein GM130 or early endosome protein EEA1 for confocal imaging. Colocalization relationship was analyzed by calculating the Pearson–Spearman correlation coefficient. Bars, 10 μm.

Golgi-localized membrane protein that contains tyrosine- and dilysine-based Golgi retention motifs at the C-terminal cytosolic tail for interaction with COPI (Sato *et al.*, 2001). Truncation of the C-terminal 10 residues of Rer1p (Rer1p-Δ10) results in mislocalization of Rer1p to the vacuole (Sato *et al.*, 2001). As shown in Figure 6D, after attachment of the KXD/E motif to the C-terminus of the mislocalized Rer1p-Δ10, the GFP-Rer1p-Δ10-RNIKCD recovered to punctate GFP signals in the wild-type strain RSY255 under permissive and restrictive temperatures. However, the localization of GFP-Rer1p-Δ10-RNIKCD was shifted to the vacuole in the coatomer mutant *sec27-1* under permissive and restrictive temperatures (Figure 6D). These results are consistent with a previous study showing the vacuole localization of GFP-Rer1p in a COPI mutant and further support the conserved function of the KXD/E motif in COPI binding and Golgi retention in yeast (Sato *et al.*, 2001).

Knockdown of COPI coatomer results in mislocalization of EMPs in plants

To investigate further the relationship between COPI and Golgi-localized EMPs containing the KXD/E COPI interaction motif, we next used an RNAi approach to generate transgenic *Arabidopsis* plants expressing hairpin RNAi fragments against ε-COP under the control of a dexamethasone (DEX)-inducible promoter (Figure 7A). The

hairpin RNAi construct, which is designed to target the conserved region of two *Arabidopsis* ε-COP homologues, can effectively knock down the expression of both ε-COP homologues in *Arabidopsis* protoplasts and transgenic plant as assessed by Western blot analysis and reverse transcription-PCR (RT-PCR) detection, respectively (Supplemental Figure S6). After DEX induction, the DEX inducible ε-COP RNAi seedlings were found to be lethal, proving the essential function of COPI in plant growth and development (Supplemental Figure S6). Transgenic *Arabidopsis* plants expressing AtEMP12-GFP-RNIKCD, a Golgi-localized fluorescent fusion protein with effective COPI interaction motif at the C-terminus (Gao *et al.*, 2012), were next selected to cross into the DEX-inducible ε-COP RNAi plant for subsequent study. As shown in Figure 7B, without DEX treatment, AtEMP12-GFP-RNIKCD showed clear punctate GFP signals corresponding to the typical Golgi localization pattern (Gao *et al.*, 2012, 2014a). However, strong vacuolar GFP signals were detected after knockdown of ε-COP by DEX induction, suggesting mislocalization of AtEMP12-GFP-RNIKCD to the vacuole (Figure 7B). These results are consistent with previous transient expression results showing mislocalization of AtEMP12-GFP to post-Golgi compartments due to blockage of the COPI interaction motif KXD/E (Gao *et al.*, 2012) and thus further prove the COPI dependence of AtAtEMP12 Golgi retention in plants.
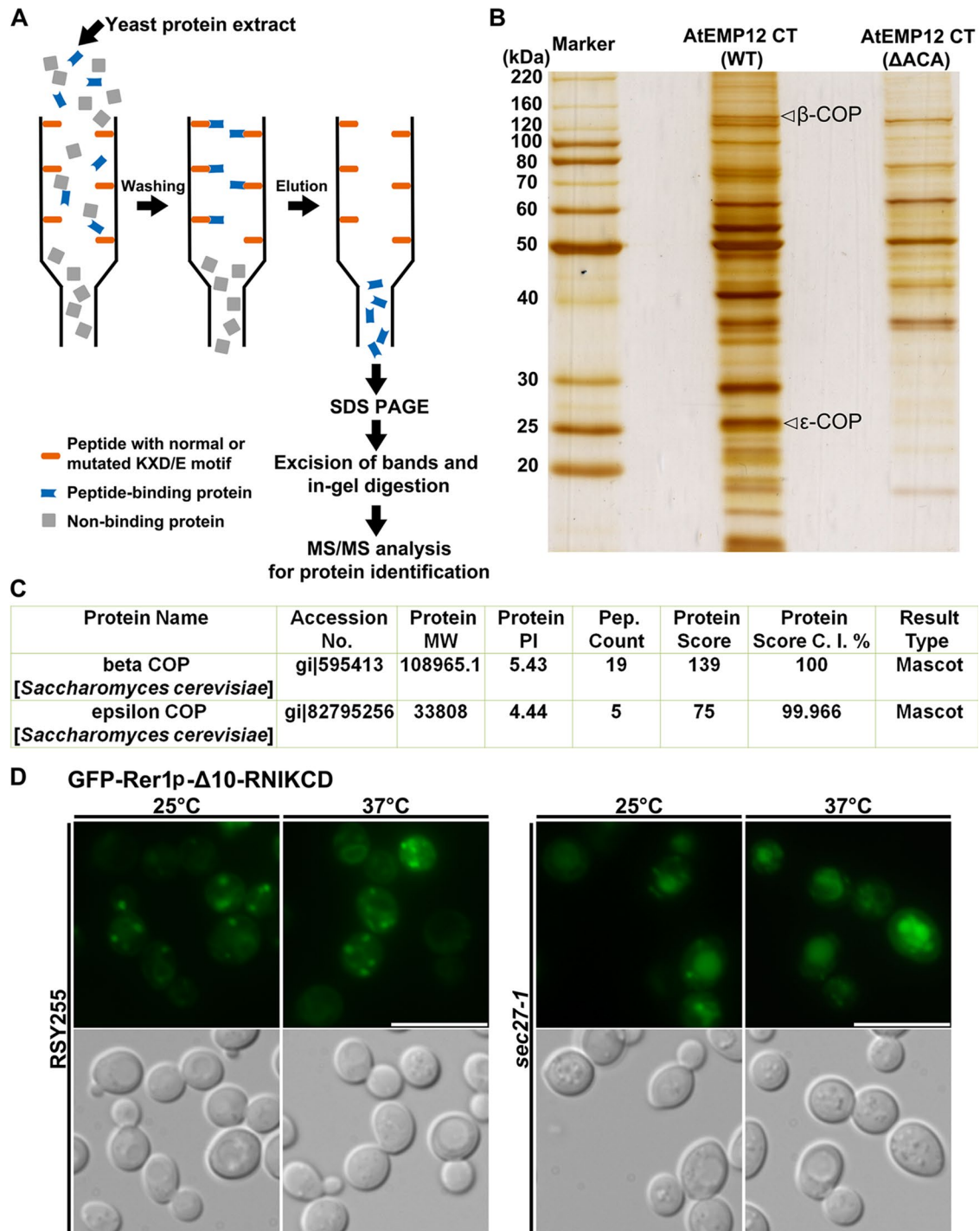
FIGURE 6: KXD/E motif shows COPI interaction in yeast. (A) The pull-down assay. Protein from the yeast strain AH109 was extracted and incubated with resins conjugated with the normal or mutated peptides corresponding to the CT of AtEMP12. After washing and elution, the eluted proteins were separated by SDS–PAGE, followed by silver staining and MS/MS analysis. (B) The silver-stained gel after pull-down assay. Arrowheads indicated COPI coat proteins identified in this experiment. (C) Search results of the COPI coat proteins in the MS/MS analysis. C.I., confidence interval; MW, molecular weight in daltons; PI, isoelectric point. (D) Localization of GFP-Rer1p-Δ10-RNIKCD in wild-type strain RSY255 and *sec27-1* mutant yeast under permissive (25°C) and restrictive (37°C) temperatures. Bars, 10 µm.

Knockdown of COPI coatomer causes morphological changes in the Golgi apparatus of plants

To investigate the effects of COPI coatomer knockdown at the ultra-structural level, we performed transmission electron microscopic (TEM) analysis of ultrathin sections of ε-COP RNAi seedlings pro-cessed by high-pressure freezing/freeze substitution. In root tip cells, one of the obvious changes observed under TEM was the re-duction in the number of cisternae per Golgi stack in the DEX-treated ε-COP RNAi plants (Figure 8). Compared with noninduced plants, in which the Golgi apparatus usually contained around five
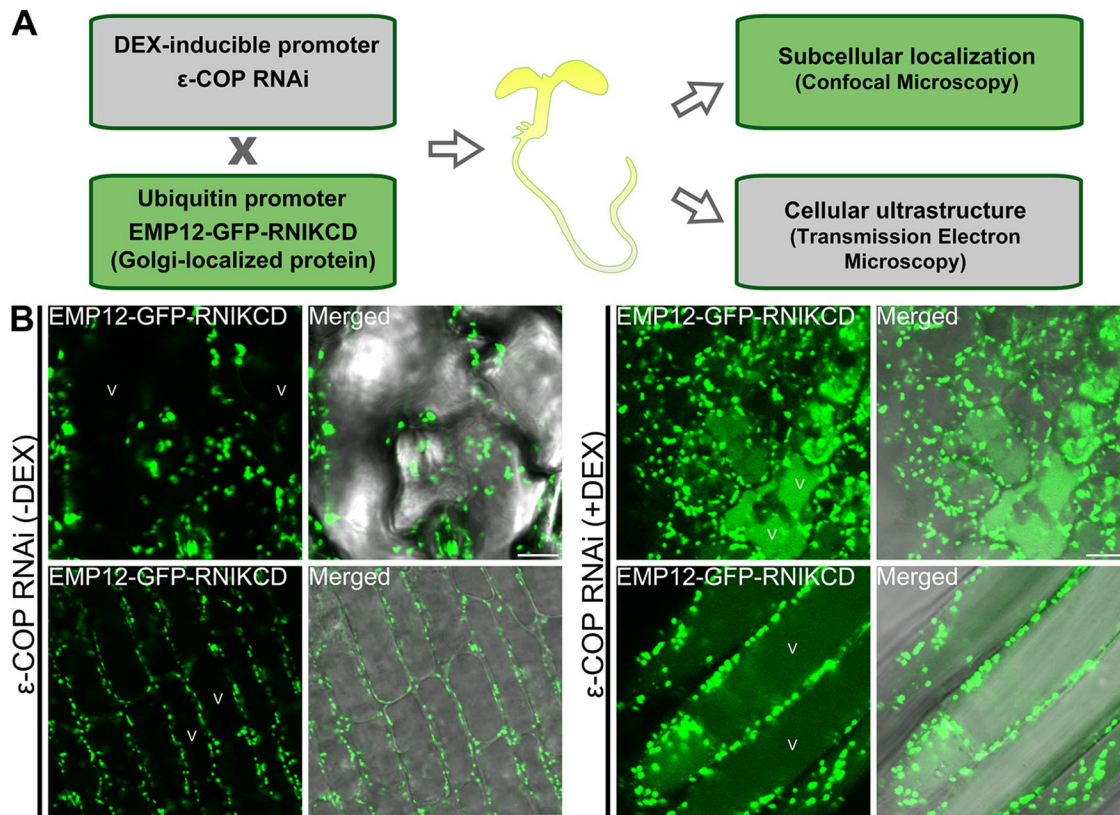
FIGURE 7: Knockdown of ε-COP results in mislocalization of the Golgi-localized AtEMP12-GFP-RNIKCD. (A) The experimental flow of this study. Transgenic plants of DEX-inducible ε-COP RNAi and transgenic plants expressing Golgi-localized AtEMP12-GFP-RNIKCD were generated and crossed. The fluorescence of the GFP signals and the ultrastructural morphology of the crossed plants were examined by confocal microscopy and TEM, respectively. (B) Seeds of AtEMP12-GFP-RNIKCD under background of DEX-inducible ε-COP RNAi were germinated on the plates with or without DEX inducer, followed by confocal observation. v, vacuoles. Bars, 10 μm.

cisternae, the Golgi apparatus in the DEX-treated plants had a significant reduction in the number of cisternae to around three or four (Figure 8). In addition to this alteration of Golgi morphology, the DEX-treated plants also contained many abnormal vesicle clusters that resemble secretory vesicles near the Golgi remnants, and the sizes of those vesicles varied from ~100 to 250 nm (Figure 8 and Supplemental Figure S7).

In the cells of cotyledons after DEX treatment, however, we found it difficult to detect a normal Golgi with typical architecture. Instead, the Golgi in this cell type became much more fragmented (Figure 9). To find out whether AtEMP12 was still located to these drastically fragmented Golgi remnants, we performed immunogold labeling with AtEMP12-specific antibodies (Gao et al., 2012). The results obtained revealed that anti-AtEMP12 labeling could still be found in the fragmented Golgi structures, possibly ER–Golgi hybrids (Figure 9). In addition, we also observed gold particle labeling on MVBs (Figure 9), which is consistent with our previous results implicating MVBs on the pathway to vacuolar degradation of AtEMP12 upon mutation of the KXD/E motif (Gao et al., 2012).

KXD/E motif in other membrane proteins

We next performed an in silico bioinformatic search in different organisms to identify membrane proteins that contain the KXD/E motif in their cytosol-located C-terminal tail. This search identified ~200 membrane proteins in *Arabidopsis*, humans, and yeast all containing a C-terminal KXD/E motif in their cytosolic tails

(Supplemental Table S1). The table in Figure 10A lists some examples of these newly identified membrane proteins containing C terminal–located KXD/E motifs. We selected At1g61670, an integral membrane protein predicted to have a long lumenal N-terminus harboring a signal peptide (SP), followed by seven transmembrane domains and a short cytosolic C-terminus, and then made an N-terminal GFP fusion for localization studies (Figure 10B). GFP-At1g61670 was correctly expressed as an intact fusion protein in *Arabidopsis* protoplasts as determined by Western blot analysis with GFP antibody (Supplemental Figure S3). Albeit with some faint ER signal, GFP-At1g61670 fusion showed clear punctate signals that largely colocalized with the Golgi marker ManI-mRFP and were distinct from the PVC marker mRFP-VSR2 (Figure 10C). These results indicate that the KXD/E motif may perform a general COPI-interaction function for membrane proteins other than EMPs.

DISCUSSION

Localizations of EMPs among different eukaryotic organisms
In this study, we provided comprehensive data showing that the position of a GFP tag markedly affects the localization of EMPs in different eukaryotic organisms. We found that irrespective of the type of expression system, the N-terminal GFP-fused EMPs always showed Golgi localization, whereas C-terminal GFP-fused EMPs were mistargeted to post-Golgi compartments. Our results help to solve the controversy surrounding conclusions made in different
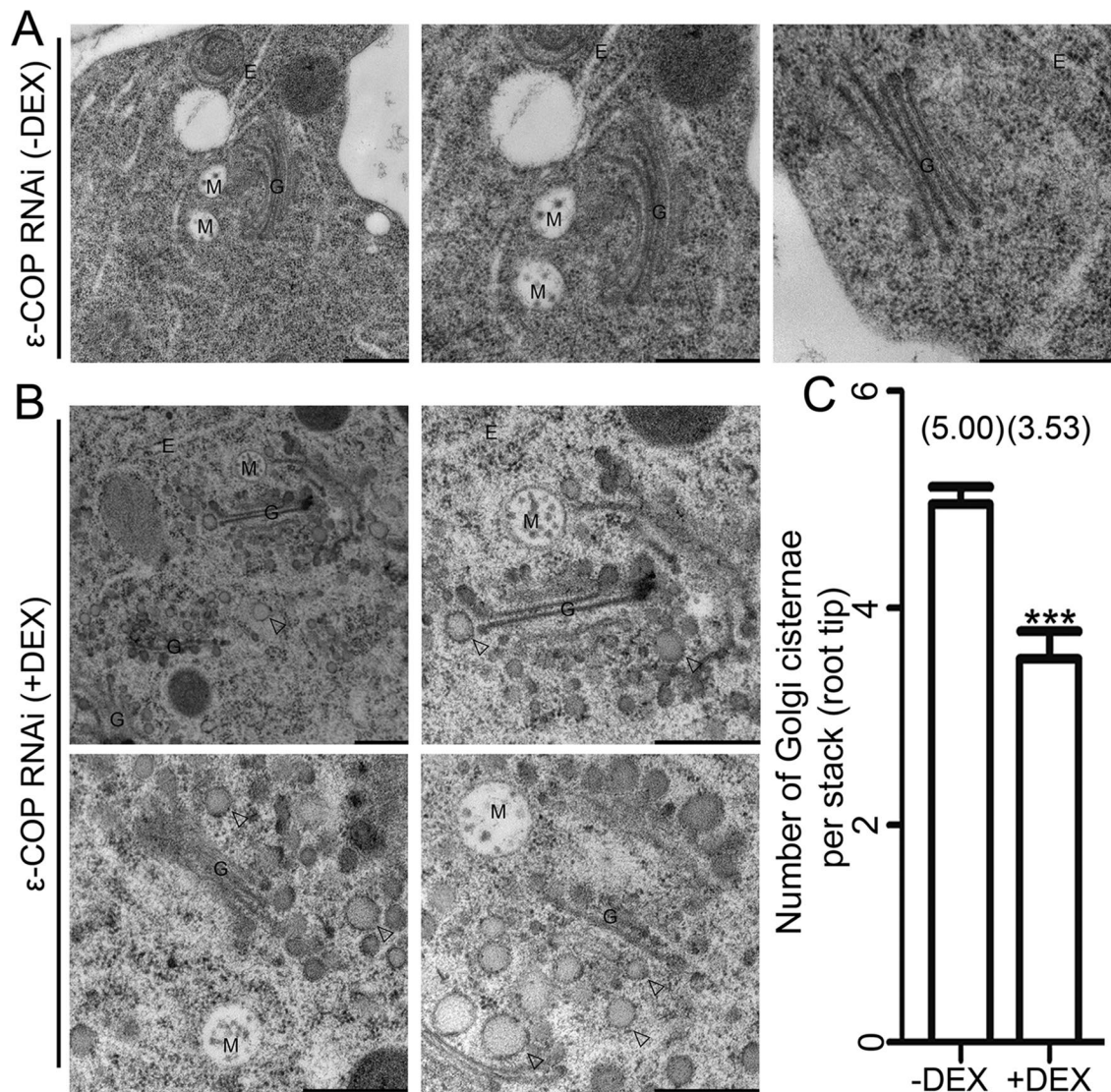
FIGURE 8: Effects of COPI RNAi on Golgi morphology in root tip cells. (A, B) Ultrathin sections were prepared from high-pressure frozen/freeze-substituted root tips of transgenic DEX-induced ε-COP RNAi seedlings grown on the plates with or without DEX for 4 d. E, endoplasmic reticulum; G, Golgi; M, multivesicular body. Bars, 500 nm. (C) Statistical analysis of the number of Golgi stacks as shown in A and B. The numbers inside the parentheses are the average number of Golgi stacks. Significant difference of Golgi stack number between wild-type and DEX-induced εCOP RNAi seedlings was analyzed using the two-tailed paired t test (***$p < 0.001$).

reports regarding to the subcellular localizations of EMPs. For example, C-terminal GFP-fused TMN2-GFP was shown to localize to early endosomes and the vacuole in yeast (Aguilar *et al.*, 2010). Similarly, in mammalian cells, C-terminal GFP-tagged TM9SF1-GFP localized to autophagosomes and lysosomes (He *et al.*, 2009). The post-Golgi localization of the EMPs in these studies is most likely due to the C-terminal fusion of the GFP tag, which blocks the interaction between KXD/E motifs and COPI coatomers and thus causes mislocalization of EMPs. Mislocalizations of the EMPs with mutations of KXD/E motif further proved the essential function of the KXD/E motif in mediating Golgi localization of EMPs.

Correct Golgi targeting should be essential for the normal functions of EMPs. A direct approach to prove this hypothesis is to perform mutant complementation assays by expression of either GFP-EMPs or EMPs-GFP in mutants harboring mutations in the corresponding EMP allele to see which form of GFP fusion can restore the mutant phenotype. Indeed, a previous study using this kind of complementation assay showed that C-terminal GFP-fused Rer1p-GFP, which mislocalizes to the vacuole due to the blockage of the C-terminal COPII-interaction signals by the GFP tag, cannot complement the yeast *rer1p* mutant (Sato *et al.*, 2001). In addition, N-terminal GFP-fused GFP-AtEMP12, but not the C-terminal fused variant, correctly performs its salt stress–related function in *Arabidopsis* (unpublished data). Clearly, more detailed mechanistic research into EMP function, as well as into the correlation between the function and subcellular localizations of EMPs, is needed. Only then will we be able to better understand the physiological function of the conserved KXD/E motif in EMPs.

KXD/E is a conserved Golgi retention signal that interacts with COPI

The binding of the KXD/E motif with plant coatomer demonstrated in our previous report (Gao *et al.*, 2012) and with yeast coatomer as discovered in this study demonstrates the conserved function of
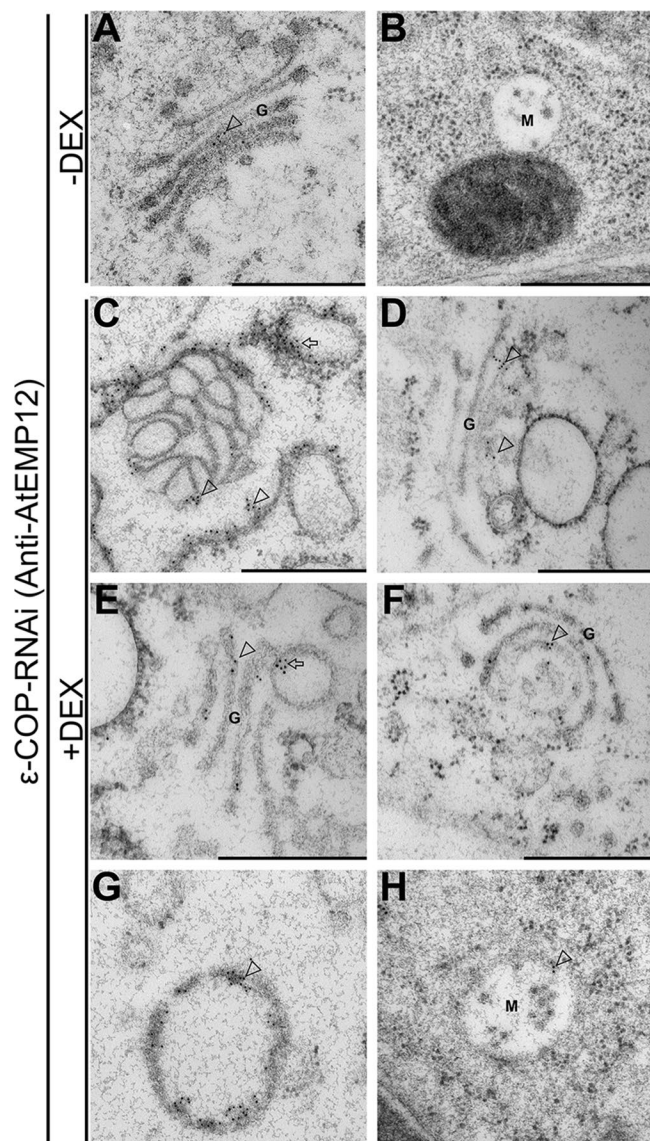
FIGURE 9: Effects of COPI RNAi on Golgi morphology in cotyledon cells. Ultrathin sections were prepared from high-pressure frozen/freeze-substituted samples of ε-COP RNAi seedlings without DEX treatment (A, B) or with DEX induction (C–H), followed by immunogold labeling using AtEMP12 antibodies. Bars, 500 nm.

KXD/E in COPI binding. Further evidence in support of a conserved function of KXD/E in Golgi retention comes from the result showing Golgi restoration of a truncated form of Rer1p, which lacks the COPI interaction motif, after adding a KXD/E motif. In addition, the Golgi retention of the KXD/E motif is COPI dependent, since the original Golgi-localized GFP-Rer1p-Δ10-RNIKCD mislocalizes to the vacuole in the yeast coatomer mutant *sec27-1*. These results are consistent with previous studies showing that dysfunction of COPI function by temperature-sensitive mutations of coatomers in yeast generally led to mislocalization and vacuolar targeting of Golgi-resident membrane proteins (Sato et al., 2001; Tu et al., 2008). Furthermore, we showed that knockdown of COPI components by inducible RNAi in transgenic *Arabidopsis* plants causes mislocalization of the Golgi-localized AtEMP12-GFP-RNIKCD fusion to the vacuole (Figure 11), proving the COPI-dependent Golgi retention of EMPs in plants. Collectively these results strongly suggest a conserved function of

the KXD/E motif in COPI binding and Golgi retention in different organisms.

In addition to EMPs, the KXD/E motif in cytosolic C-termini is found in other membrane proteins from different organisms, including *Arabidopsis,* yeast, and human (Figure 10A; Gao et al., 2014a). It would therefore be interesting to test the possible conserved functions of the KXD/E motif in COPI interaction and Golgi retention for other membrane proteins. Golgi localization of the N-terminal GFP fused GFP-At1g61670 in plants as shown in this study reveals the possibility of a general Golgi retention function of the KXD/E motif for other membrane proteins in addition to EMPs. Thus the conserved function of the KXD/E motif may provide useful information to guide the subcellular localization and functional study of membrane proteins that contain this motif in their C-terminus. More detailed subcellular localization studies of these newly identified KXD/E motif–containing membrane proteins using both N-terminal and C-terminal GFP fusions, as well as immunocyto-chemical use of specific antibodies, will be conducted in the future.

Crucial function of COPI in maintaining cellular function and morphology in early secretory pathway

In addition to its well-known function in mediating retrograde transport from the Golgi back to the ER, COPI also performs functions in mediating intra-Golgi trafficking. Regarding the event of intra-Golgi trafficking for cargo proteins, however, there exist two typical models: vesicular transport and cisternal maturation. The vesicular transport model predicts that Golgi cisternae are long-lived and stable structures that retain their resident proteins, whereas secretory cargo proteins are transported by vesicles from one cisterna to the next. However, the cisternal maturation model predicts that cisternae are transient structures that form de novo and mature from *cis* to *trans* by acquiring and then losing specific Golgi-resident proteins, whereas secretory cargo proteins traverse the Golgi apparatus by remaining within the maturing cisternae. Studies in yeast via live imaging have made the cisternal maturation model more popular (Losev et al., 2006; Matsuura-Tokita et al., 2006). Regarding the functional diversity of COPI, recent electron tomography studies in *Arabidopsis* and algal cells identified two structurally distinct types of COPI vesicles, termed COPIa and COPIb vesicles, respectively (Donohoe et al., 2007). COPIa vesicles have a lightly stained content, bud exclusively from *cis*-Golgi cisternae, and occupy the ER–Golgi interface, whereas COPIb vesicles have a darkly stained content, bud exclusively from medial- and *trans*-Golgi cisternae, and are confined to the space around these cisternae (Donohoe et al., 2007). We propose that after synthesis in the ER, EMPs are first transported from ER to *cis*-cisternae of Golgi via COPII vesicles and then reach the medial and *trans* sides of the Golgi, from which EMPs preferentially interacts with COPIb to be recycled from medial and *trans* sides back to the *cis* side of the Golgi apparatus (Figure 11; Gao et al., 2014a).

In addition to functioning as part of the retention machinery for membrane proteins as discussed, COPI is also important for maintaining normal cellular function and organelle morphology in the early secretory pathway. In yeast, the COPI coatomer *sec21* mutant exhibits early Golgi-specific glycosylation defects and significant perturbation of early but not late Golgi structure (Gaynor and Emr, 1997). In mammalian cells, disruption of COPI function also leads to significant morphological changes in Golgi structure. For example, disruption the function of temperature-sensitive ε-COP at the nonpermissive temperature in the CHO cell line causes complete disassociation of the Golgi apparatus into vesicles and tubules (Guo et al., 1994), whereas depletion of β-COP results in
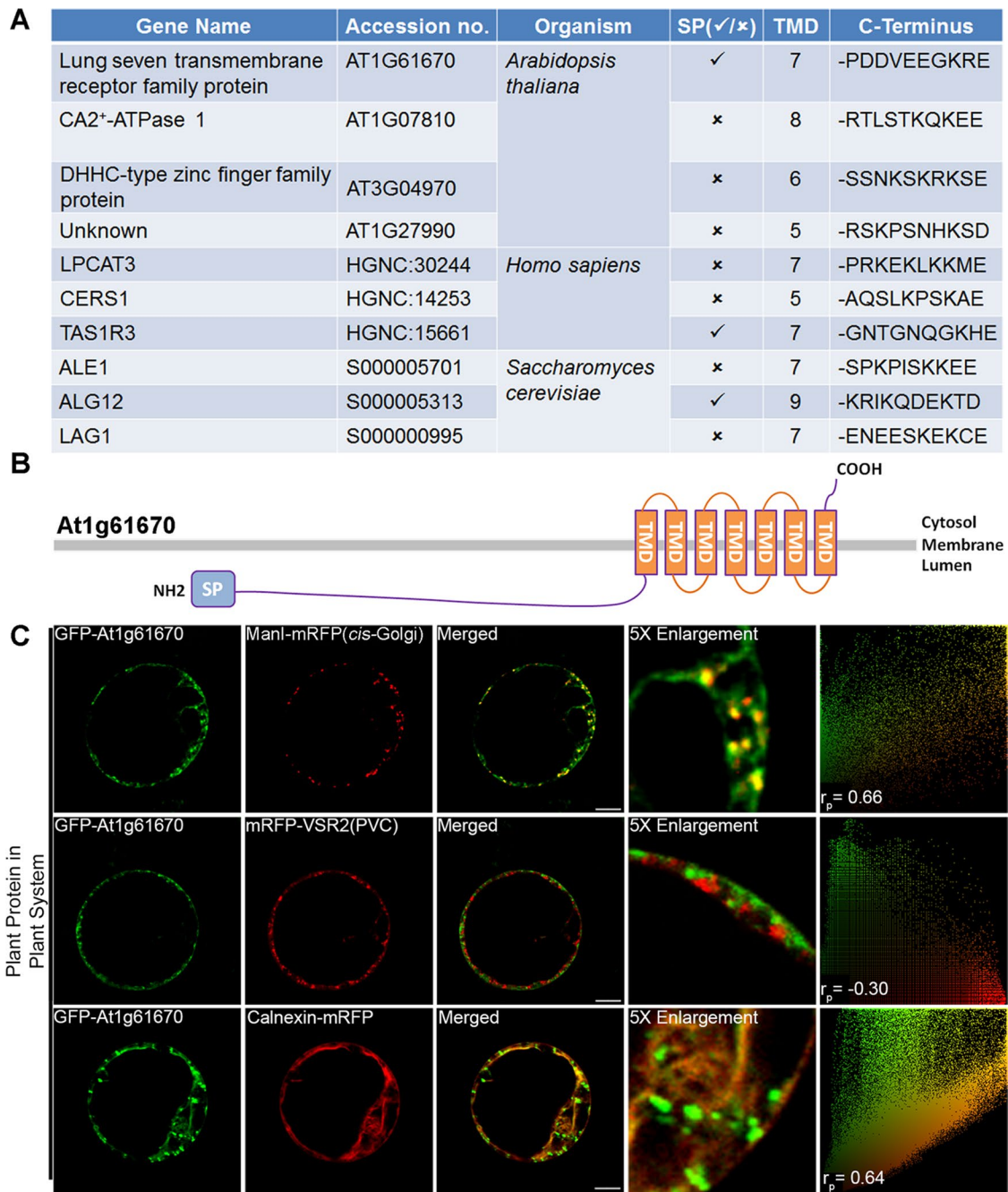
FIGURE 10: Other proteins carrying KXD/E motif at C-terminus can localize to Golgi. (A) Representative membrane proteins containing the KXD/E motif in different organisms. (B) Schematic topology of At1g61670 predicted by TMHMM 2.0. (C) Coexpressions of GFP-At1g61670 and At1g61670-GFP with *cis*-Golgi marker ManI-mRFP, PVC marker mRFP-VSR2, or ER marker calnexin-mRFP were performed in *Arabidopsis* protoplasts. Confocal images of transfected cells were collected after 12–14 h of transfection. Colocalization relationship was measured using Pearson–Spearman correlation. Bars, 10 μm.

fragmentation of the Golgi complex and formation of globular compartments containing markers of the ER-Golgi intermediate compartment, Golgi, TGN, and recycling endosomes (Styers *et al.*, 2008). In plants, the best observation of an effect of COPI dysfunction in Golgi morphology has come from the study of the effect of brefeldin A (BFA) on tobacco BY-2 cells (Ritzenthaler *et al.*, 2002). BFA is a fungal toxin that inhibits the activity of guanine nucleotide exchange factor of the Arf GTPases and thus inhibits the membrane recruitment of coatomer and the formation of COPI vesicles

(Donaldson *et al.*, 1992). BFA treatment causes a rapid loss of coatomer from Golgi membrane and leads to severe morphological changes in Golgi architecture, including loss of distinct Golgi stacks, aggregations of Golgi stack remnants and large numbers of secretory vesicles surrounding the Golgi stacks, which are so-called BFA compartments, and finally formation of ER–Golgi hybrid compartment (Ritzenthaler *et al.*, 2002). Here we demonstrated that knockdown of coatomer by DEX-inducible ε-COP RNAi in plants causes a dramatic reduction in the number of Golgi cisternae per
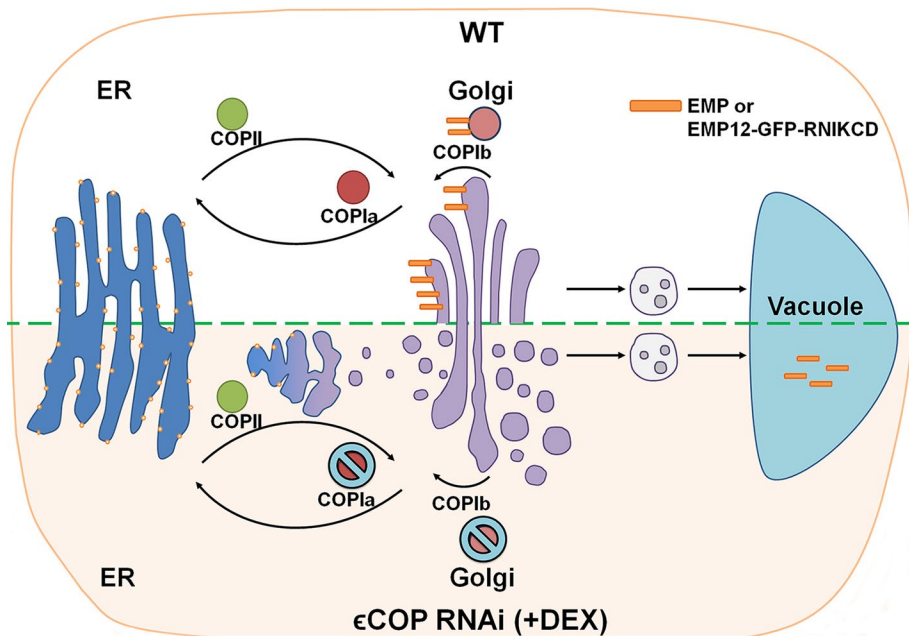
FIGURE 11: Working model of COPI-dependent targeting of EMP proteins. The KXD/E motif at the C-terminus of EMP protein may interact preferentially with COPIb and mediate its Golgi retention (top). On knockdown of ε-COP, EMPs lose their Golgi localization and mistarget to vacuole for degradation (bottom). In addition, knockdown of ε-COP results in dramatic changes in Golgi morphology, such as reduction in the number of Golgi stacks and accumulation of abnormal vesicles around the Golgi (bottom).

stack, formation of clusters of secretory vesicles surrounding the Golgi remnants, drastic fragmentation of Golgi apparatus, and formation of ER–Golgi hybrids. These phenotypes under the electron microscope seem to mimic the effects of BFA treatment and thus further prove the essential role of COPI in maintaining the normal morphology and function of the ER and Golgi in the early secretory pathway. Our DEX-inducible coatomer RNAi plants will prove to be useful materials for further studies into the function of COPI in intracellular protein trafficking, as well as into the other physiological function of COPI in plant development.

MATERIALS AND METHODS
Plasmid construction
For constructs for transgenic plant generation, AtEMP12-GFP-RNIKCD was amplified from a construct of AtEMP12-GFP and cloned into the pBI121 backbone (Clough and Bent, 1998). To generate the ε-COP RNAi construct, a conserved region with an ~400–base pair sequence of the two ε-COP homologues predicted using MatchPoint (www.csiro.au/en/Research/Farming-food/Innovation-and-technology-for-the-future/Gene-technology/RNAi) was amplified as two fragments and inserted into the hairpin RNAi vector pHANNIBAL. The hairpin FREE1 RNAi fragment was then subcloned into the pTA7002 vector under the DEX-inducible promoter (Aoyama and Chua, 1997).

All constructs used for transient expression in protoplasts were generated by PCR amplification and cloned into pBI221 vector having the cauliflower mosaic virus 35S promoter, GFP coding sequence, and nopaline synthase terminator (Miao *et al.*, 2008). Signal peptide sequences for making GFP fusion constructs were derived from barley (*Hordeum vulgare*) proaleurain (Jiang and Rogers, 1998) or native signal peptide sequences of EMP homologues according to SignalP 3.0 Server prediction (www.cbs.dtu.dk/services/SignalP/).

All EMP homologues constructs used for transfection in HEK293a cells were PCR amplified and cloned into pEGFPC1 or pEG-FPN1 vectors containing cauliflower mosaic virus 35S promoter, GFP coding sequence, and TK pA terminator. Signal peptide sequences for generating GFP fusion constructs were derived from HsTM9SF4 or native signal peptide sequences of EMP homologues as predicted by SignalP 3.0 Server. Construct confirmation was done using restriction mapping and DNA sequencing. Protein topology prediction was made by TMHMM Server 2.0 (www.cbs.dtu.dk/services/TMHMM/). The primer list for plasmid generation is given in Supplemental Table S2.

Transgenic plant generation and expression systems
Procedures for transgenic *Arabidopsis thaliana* plant generation expressing XFP fusion proteins using techniques of floral dipping were as previously described (Clough and Bent, 1998; Tse *et al.*, 2004). Transgenic *Arabidopsis* expressing XFP-fused Golgi At-EMP12-GFP-RNIKCD were crossed with *Arabidopsis* plants expressing DEX-inducible COPI hairpin RNAi.

Procedures of transient expression using protoplasts prepared from *Arabidopsis* suspension culture cells were performed according to our established protocol (Miao and Jiang, 2007). Transfection and subsequent immunofluorescence studies using HEK293a cells were as previously described (Ding *et al.*, 2014). Cells after 12–14 h of transfection were washed with phosphate-buffered saline and fixed with 4% paraformaldehyde for immunolabeling and confocal imaging. Transformation methods for yeast using strain RSY255, BY4741, or *sec27-1* have been described (Elble, 1992). After overnight culture in drop-out medium, culture in yeast extract/peptone/dextrose (YEPD) medium was prepared and incubated at 25°C for 3–4 h for fluorescence microscopy. Temperature shift was performed for 30 min under restrictive temperature before fluorescence microscope observation.

In vitro binding assay
Pull-down assay and liquid chromatography-MS/MS analysis were essentially carried out according to the procedures described previously (Gao *et al.*, 2012). Synthetic peptides (GenScript, Piscataway, NJ) corresponding to AtAtEMP12 C-terminal cytosolic tail were coupled via their N-terminal NH_2 group to cyanogen bromide–activated Sepharose 4B. Soluble yeast proteins from strain AH109 were extracted for the binding assay with peptide-coupled Sepharose beads. Proteins were separated by SDS–PAGE and subjected to liquid chromatography-MS/MS analysis.

Fluorescence microscopy and confocal microscopy
Protoplasts electroporated with genes of interest were incubated for 12–17 h before microscopic observation. Transfected HEK293a cells were incubated for 12–17 h before fixation using 4% paraformaldehyde. The immunolabeling process for HEK293a cells was as previously described (Ding *et al.*, 2014). Organelle marker antibodies, including GM130, EEA1, and LAMP1, were used as primary

antibody. Anti-TM9SF4 antibody was purchased from Abcam (Cambridge, MA; ab98879).

For confocal microscope observation of plant protoplasts and HEK293a cells, either an Olympus FluoView FV1000 confocal microscope (Olympus, Tokyo, Japan) with a 60× water lens or a Leica SP8 confocal microscope (Leica, Wetzlar, Germany) with a 60× water lens was used. Fluorescence microscope observation in yeast was conducted using a Zeiss Axioskop microscope (Carl Zeiss, Jena, Germany) equipped with Zeiss Plan-Neofluar 100×/1.30 numerical aperture oil objective lens. Details about settings of image collection and Photoshop processing (Adobe, San Jose, CA) were as previously described (Gao et al., 2012). The Pearson–Spearman correlation for colocalization relationships was calculated using ImageJ (National Institutes of Health, Bethesda, MD) and PSC plug-in as described previously (French et al., 2008).

Protein preparation and immunoblot analysis

To prepare cell extracts from protoplasts, transformed protoplasts were suspended in the lysis buffer containing 25 mM Tris-HCl, pH 7.5, 150 mM NaCl, 1 mM EDTA, and 1× Protease Inhibitor Cocktail (Cat No. 05056489001; Roche Applied Science). The protoplasts were further lysed by passage through a 1-ml syringe with needle and then spun at $600 \times g$ for 3 min to remove intact cells and large cellular debris. The supernatant total cell extracts were then centrifuged at $100,000 \times g$ for 30 min at 4°C; the supernatant and pellet were assigned as soluble and membrane fractions, respectively. To prepare cell extracts from mammalian cells, transfected HEK293a cells were lysed in the buffer (10 mM Tris-HCl, pH 7.5, 150 mM NaCl, 5 mM EDTA, 0.1% SDS, 1% Triton X-100, 1% deoxycholate, and 1× Complete Protease Inhibitor Cocktail). Proteins were separated by SDS–PAGE and analyzed by immunoblotting.

Electron microscopy

General procedures for TEM sample preparation, ultrathin sectioning, and immunogold labeling have been described (Gao et al., 2012, 2014b, 2015). Root tips of wild-type or inducible COPI RNAi transgenic Arabidopsis plants were germinated and grown under 30 mM DEX for 5 d. The 5-d-old plants were cut and frozen using a PACT2 high-pressure freezer (Leica). The samples were then freeze substituted using dry acetone with 0.1% uranyl acetate in an AFS freeze substitution unit at −85°C (Leica), followed by infiltration with HM20, embedding, and ultraviolet polymerization at −35°C. Immunogold labeling was performed with primary AtAtEMP12 antibodies at 40 mg/ml and gold-coupled secondary antibodies at 1:50 dilution. TEM observation was completed using a Hitachi H-7650 transmission electron microscope with a charge-coupled device camera functioning at 80 kV (Hitachi High-Technologies, Tokyo, Japan).

REFERENCES

Aguilar PS, Frohlich F, Rehman M, Shales M, Ulitsky I, Olivera-Couto A, Braberg H, Shamir R, Walter P, Mann M, et al. (2010). A plasma-membrane E-MAP reveals links of the eisosome with sphingolipid metabolism and endosomal trafficking. Nat Struct Mol Biol 17, 901–908.

Aoyama T, Chua NH (1997). A glucocorticoid-mediated transcriptional induction system in transgenic plants. Plant J 11, 605–612.

Barlowe C, Orci L, Yeung T, Hosobuchi M, Hamamoto S, Salama N, Rexach MF, Ravazzola M, Amherdt M, Schekman R (1994). COPII: a membrane coat formed by Sec proteins that drive vesicle budding from the endoplasmic reticulum. Cell 77, 895–907.

Benghezal M, Cornillon S, Gebbie L, Alibaud L, Bruckert F, Letourneur F, Cosson P (2003). Synergistic control of cellular adhesion by transmembrane 9 proteins. Mol Biol Cell 14, 2890–2899.

Chluba-de Tapia J, de Tapia M, Jaggin V, Eberle AN (1997). Cloning of a human multispanning membrane protein cDNA: evidence for a new protein family. Gene 197, 195–204.

Clough SJ, Bent AF (1998). Floral dip: a simplified method for Agrobacterium-mediated transformation of Arabidopsis thaliana. Plant J 16, 735–743.

Contreras I, Yang Y, Robinson DG, Aniento F (2004). Sorting signals in the cytosolic tail of plant p24 proteins involved in the interaction with the COPII coat. Plant Cell Physiol 45, 1779–1786.

Cornillon S, Pech E, Benghezal M, Ravanel K, Gaynor E, Letourneur F, Bruckert F, Cosson P (2000). Phg1p is a nine-transmembrane protein superfamily member involved in dictyostelium adhesion and phagocytosis. J Biol Chem 275, 34287–34292.

Cosson P, Letourneur F (1994). Coatomer interaction with di-lysine endoplasmic reticulum retention motifs. Science 263, 1629–1631.

Ding Y, Wang J, Chun Lai JH, Ling Chan VH, Wang X, Cai Y, Tan X, Bao Y, Xia J, Robinson DG, Jiang L (2014). Exo70E2 is essential for exocyst subunit recruitment and EXPO formation in both plants and animals. Mol Biol Cell 25, 412–426.

Donaldson JG, Finazzi D, Klausner RD (1992). Brefeldin A inhibits Golgi membrane-catalysed exchange of guanine nucleotide onto ARF protein. Nature 360, 350–352.

Donohoe BS, Kang BH, Staehelin LA (2007). Identification and characterization of COPIa- and COPIb-type vesicle classes associated with plant and algal Golgi. Proc Natl Acad Sci USA 104, 163–168.

Elble R (1992). A simple and efficient procedure for transformation of yeasts. BioTechniques 13, 18–20.

French AP, Mills S, Swarup R, Bennett MJ, Pridmore TP (2008). Colocalization of fluorescent markers in confocal microscope images of plant cells. Nat Protoc 3, 619–628.

Froquet R, Cherix N, Birke R, Benghezal M, Cameroni E, Letourneur F, Mosch HU, De Virgilio C, Cosson P (2008). Control of cellular physiology by TM9 proteins in yeast and Dictyostelium. J Biol Chem 283, 6764–6772.

Gao C, Cai Y, Wang Y, Kang BH, Aniento F, Robinson DG, Jiang L (2014a). Retention mechanisms for ER and Golgi membrane proteins. Trends Plant Sci 19, 508–515.

Gao C, Luo M, Zhao Q, Yang R, Cui Y, Zeng Y, Xia J, Jiang L (2014b). A unique plant ESCRT component, FREE1, regulates multivesicular body protein sorting and plant growth. Curr Biol 24, 2556–2563.

Gao C, Yu CK, Qu S, San MW, Li KY, Lo SW, Jiang L (2012). The Golgi-localized Arabidopsis endomembrane protein12 contains both endoplasmic reticulum export and Golgi retention signals at its C terminus. Plant Cell 24, 2086–2104.

Gao C, Zhuang X, Cui Y, Fu X, He Y, Zhao Q, Zeng Y, Shen J, Luo M, Jiang L (2015). Dual roles of an Arabidopsis ESCRT component FREE1 in regulating vacuolar protein transport and autophagic degradation. Proc Natl Acad Sci USA 112, 1886–1891.

Gaynor EC, Emr SD (1997). COPI-independent anterograde transport: cargo-selective ER to Golgi protein transport in yeast COPI mutants. J Cell Biol 136, 789–802.

Guo Q, Vasile E, Krieger M (1994). Disruptions in Golgi structure and membrane traffic in a conditional lethal mammalian cell mutant are corrected by epsilon-COP. J Cell Biol 125, 1213–1224.

He P, Peng Z, Luo Y, Wang L, Yu P, Deng W, An Y, Taiping Shi T, Ma D (2009). High-throughput functional screening for autophagy-related genes and identification of TM9SF1 as an autophagosome-inducing gene. Autophagy 5, 52–60.

Huh WK, Falvo JV, Gerke LC, Carroll AS, Howson RW, Weissman JS, O'Shea EK (2003). Global analysis of protein localization in budding yeast. Nature 425, 686–691.

Jiang L, Rogers JC (1998). Integral membrane protein sorting to vacuoles in plant cells: evidence for two pathways. J Cell Biol 143, 1183–1199.

Le Coadic M, Froquet R, Lima WC, Dias M, Marchetti A, Cosson P (2013). Phg1/TM9 proteins control intracellular killing of bacteria by determining cellular levels of the Kil1 sulfotransferase in Dictyostelium. PLoS One 8, e53259.

Letourneur F, Gaynor EC, Hennecke S, Demolliere C, Duden R, Emr SD, Riezman H, Cosson P (1994). Coatomer is essential for retrieval of dilysine-tagged proteins to the endoplasmic-reticulum. Cell 79, 1199–1207.

Losev E, Reinke CA, Jellen J, Strongin DE, Bevis BJ, Glick BS (2006). Golgi maturation visualized in living yeast. Nature 441, 1002–1006.

Lozupone F, Perdicchio M, Brambilla D, Borghi M, Meschini S, Barca S, Marino ML, Logozzi M, Federici C, Iessi E, et al. (2009). The human homologue of Dictyostelium discoideum phg1A is expressed by human metastatic melanoma cells. EMBO Rep 10, 1348–1354.

Matsuura-Tokita K, Takeuchi M, Ichihara A, Mikuriya K, Nakano A (2006). Live imaging of yeast Golgi cisternal maturation. Nature 441, 1007–1010.

Miao Y, Jiang L (2007). Transient expression of fluorescent fusion proteins in protoplasts of suspension cultured cells. Nat Protoc 2, 2348–2353.

Miao Y, Li KY, Li HY, Yao X, Jiang L (2008). The vacuolar transport of aleurain-GFP and 2S albumin-GFP fusions is mediated by the same pre-vacuolar compartments in tobacco BY-2 and Arabidopsis suspension cultured cells. Plant J 56, 824–839.

Ritzenthaler C, Nebenfuhr A, Movafeghi A, Stussi-Garaud C, Behnia L, Pimpl P, Staehelin LA, Robinson DG (2002). Reevaluation of the effects of brefeldin A on plant cells using tobacco bright yellow 2 cells expressing Golgi-targeted green fluorescent protein and COPI antisera. Plant Cell 14, 237–261.

Sato K, Sato M, Nakano A (2001). Rer1p, a retrieval receptor for endoplasmic reticulum membrane proteins, is dynamically localized to the Golgi apparatus by coatomer. J Cell Biol 152, 935–944.

Schimmöller F, Díaz E, Mühlbauer B, Pfeffer SR (1998). Characterization of a 76 kDa endosomal, multispanning membrane protein that is highly conserved throughout evolution. Gene 216, 311–318.

Styers ML, O'Connor AK, Grabski R, Cormet-Boyaka E, Sztul E (2008). Depletion of beta-COP reveals a role for COP-I in compartmentalization of secretory compartments and in biosynthetic transport of caveolin-1. Am J Physiol Cell Physiol 294, C1485–C1498.

Tse YC, Mo B, Hillmer S, Zhao M, Lo SW, Robinson DG, Jiang L (2004). Identification of multivesicular bodies as prevacuolar compartments in Nicotiana tabacum BY-2 cells. Plant Cell 16, 672–693.

Tu L, Tai WC, Chen L, Banfield DK (2008). Signal-mediated dynamic retention of glycosyltransferases in the Golgi. Science 321, 404–407.